Preprint Title Carbon nanotube-cellulose ink for rapid liquid identification

Authors Tiago Amarante, Thiago H. R. Cunha, Claudio Laudares, Ana P. M. Barboza, Ana Carolina dos Santos, Cintia L. Pereira, Vinicius Ornelas, Bernardo R. A. Neves, Andre S. Ferlauto and Rodrigo G. Lacerda

Publication Date 09 Dec 2022

Article Type Full Research Paper

Supporting Information File 1 SuppInfo artigo tiago 09DEZ2022.docx; 679.3 KB

ORCID® iDs Ana P. M. Barboza - https://orcid.org/0000-0002-1807-971X; Ana Carolina dos Santos - https://orcid.org/0000-0002-6026-8979; Bernardo R. A. Neves - https://orcid.org/0000-0003-0464-4754; Andre S. Ferlauto - https://orcid.org/0000-0003-3056-7289; Rodrigo G. Lacerda - https://orcid.org/0000-0003-4777-7370

Carbon nanotube-cellulose ink for rapid liquid identification

Tiago Amarante [†,‡], Thiago H. R. Cunha[‡], Claudio Laudares[‡], Ana P. M. Barboza[ⁱ] , Ana Carolina dos Santos[†,‡],Cíntia L. Pereira[†,‡], Vinicius Ornelas[†,‡],Bernardo R. A. Neves[†], André S. Ferlauto[§,‡], Rodrigo G. Lacerda[†,‡]*

[†]Departamento de Física, Universidade Federal de Minas Gerais, Belo Horizonte - CEP 31270-901

[‡]CTNano-UFMG - Centro de Nanotecnologia em Nanomateriais e Grafeno, Universidade Federal de Minas Gerais, Belo Horizonte - CEP 31270-901, Belo Horizonte - CEP 31310-260

[ⁱ] Departamento de Física, Universidade Federal de Ouro Preto, Ouro Preto - CEP 35400-000

[§]Centro de Engenharia, Modelagem e Ciências Sociais Aplicadas, Universidade Federal do ABC, Santo André - CEP 09210-580

Abstract

In this work, a conductive ink based on micro fibrillated cellulose (MFC) and multi-walled carbon nanotubes (MWCNT) was used to produce transducers for rapid liquid identification. The transducers are simple resistive devices that can be easily fabricated by scalable printing techniques. We monitored the electrical response due to the interaction between a given liquid with the carbon nanotube-cellulose film over time. Using principal component analysis of the electrical response, we were able to extract robust data used to differentiate several liquid categories. We show that the proposed liquid sensor can classify different liquid systems, including organic solvents (e.g., acetone, chloroform, and alcohol) and is also able to differentiate low concentrations of glycerin in water (10-100 ppm). We have also investigated the influence of two vital liquid properties: dielectric constant and vapor pressure on the physical transduction mechanisms of MFC-MWCNT sensors, which were corroborated by independent heat flow measurements (thermogravimetric analysis). The proposed MFC-MWCNT sensor platform may help paving the way to rapid, inexpensive, and robust liquid analysis and identification.

Keywords: Carbon nanotube, fibrillated cellulose, electronic tongue, and liquid sensor

1 Introduction

The development of a new generation of smart sensors that allow monitoring of industrial processes in real-time, and of wearable and flexible devices are paradigms of the current 4.0 industry. One can envision applications such as multi-component complex liquid and gas sensors, wearables for healthcare, paper-based sensors, and electronic solutions for Smart city applications [1–5]. Another area of increasing demand is the rapid test, identification and monitoring of various liquid samples in various fields such as fuel adulteration, water quality, solvents and beverages [6–9]. Usually, liquid testing requires conventional analytical techniques, such as absorption/emission spectroscopy (AAS/AES), X-ray fluorescence spectroscopy, and inductively coupled plasma mass spectrometry (ICP-MS), which are complex, expensive and require experts to carry them out (and often require several pretreatment steps with high-cost materials) [10,11] Electronic tongue is a category of liquid sensor that could solve the problems cited. These devices comprise an array of non-specific sensors that, with an appropriate method of multiple data processing, can learn and extract the desired information, constituting one of the promising candidates for developing smart sensor technologies [12–18]. Additionally, the Internet of Things (IoT) also requires devices to be integrated into a variety of systems and different surfaces of our daily life, which demands the production of low-cost, reliable, and scaled-up production of sensors [12,13,19]. However, the lack of reproducible large-scale production of liquid sensors, besides the constant need for sensor recalibration, has hindered broader commercialization of such devices [13,20].

A wide variety of materials have been explored for liquid sensing. For instance, electrically conductive polymer composites (CPC), which are generally composed by lightweight materials comprising a conductive ingredient (e.g., carbon nanotube (CNT), graphene, graphene oxide,

and metal particles) embedded in a polymer matrix, have been extensively studied as liquid sensors [14–17,21,22]. The main idea is to combine the responsive electrical properties of carbon nanostructured materials with the polymer's distinguished mechanical properties. These composites are usually non-selective and can react to various ambient stimuli [20,22–29]. Among polymers, cellulose is the most abundant natural organic polymer on earth. It has been resurfaced recently as a smart material because of its excellent thermal-mechanical properties, biocompatibility, biodegradability, and flexibility [22,23,30,31]. Composites based on carbon nanotubes or graphene and cellulose have been reported for humidity and vapor sensing, electromagnetic shield, thermoelectric material, among others [32–38]. Recently, H. Qi *et al*. reported a liquid water sensor based on carbon nanotube-cellulose composite films [39]. Besides, graphene films deposited on cellulose paper and a graphene/cellulose composite were also reported as a solvent sensor material [30,33]. However, most of these works rely on cellulose as a paper substrate or as a thick composite film that cannot be readily expanded for large-scale production.

Ink printing technology is one of the most promising approaches to fulfill all the demands and issues described above, which naturally leads to the challenge of developing new smart-ink-based materials for several applications [1–5,12,13,40–42] Carbon nanotubes and other 1D/2D materials have been employed as ink components with great potential for a broad range of applications in flexible electronics, photoconductors, transparent conductors, gas sensors, among others [43–46]. For instance, carbon nanotube ink films have been reported as field-effect transistors, transparent conductors, gas sensors, supercapacitors, pH sensing, among others [40,41,46–54]. Different approaches to ink printing methods have been explored, such as aerosol jet, inkjet, syringe, roll-to-roll printing and stamp methods[1,40,49].

In this work, we report a sensor based on a carbon nanotube/cellulose ink that proves to be highly sensitive to various solvents, water with different impurity levels, and can

detectglycerin in water down to the 10-100 ppm range. We provide insights into the liquid detection mechanism, combining the well-known swelling mechanism of polymer composites with physicochemical characteristics such as dielectric constant, specific heat, and vapor pressure [25,55,56]. Hence, our ink-based devices could extract those characteristics even from unknown samples and mixtures. Finally, test analysis using principal component analysis (PCA) was performed in different devices and on flexible and rigid substrates, providing a step forward towards scale-up and commercialization of the technology.

2 Experimental

2.1 Materials and apparatus

Micro fibrillated cellulose (MFC) with a nominal fiber width of 50 nm and several hundred microns of length was purchased from Maine University (3.0 w% aqueous gel). Functionalized multi-walled carbon nanotubes (MWCNTs) with hydroxyl and carboxyl groups (-OH and -COOH), outer diameter between 20 to 50 nm and an average length of 5 μm were produced at CTNano/UFMG [57–59]. Morphological analysis was carried out by scanning electron microscope (SEM) in a Quanta 200 FEG™, using secondary electrons between 2-10 kV. Atomic force microscopy (AFM) was carried out on a Bruker MultiMode8 SPM using the intermittent contact mode. AC160TS silicon cantilevers, from Olympus, with typical spring constant k ~ 46 N/m, nominal radius of curvature r ~7 nm and resonant frequency ω_0 ~ 300 kHz were employed. Heat flow and weight changes of selected solvents were determined by thermogravimetric analyses (TGA) using a PerkinElmer STA 8000 equipment. Electrical measurements were performed using a lock-in (SR830 DSP Stanford Research Systems), a pre-

amplifier (model 1211 DL instruments), and a multimeter (model 2000 Keithley), which were controlled by a computer.

2.2 Conductive ink and Conductive Polymer Composite (CPC)

MWCNTs were mixed with DI-water (1% w/v) and sonicated in an ultrasonic bath for two hours. The obtained suspension was centrifuged for 5 min at 2500 RPM, and the supernatant (0.6% w/v) was reserved. MFC was dispersed in DI-water (0.5% w/v) using a Silverson homogenizer (10.000 RPM) for 10 min and then filtered through a 50 μm sieve, resulting in 0.3% w/v MFC dispersion. Finally, the two suspensions were mixed in 1:1 v/v proportion and homogenized in a Silverson homogenizer to produce the final composite conductive ink, which will be called (MFC/MWCNT). See supplementary information for details.

2.3 Electronic tongue device: Transducer and data acquisition

Transducer arrays were produced by spraying the MFC/MWCNT ink onto glass substrates using an airbrush and masking tape as a stencil, as shown in Fig. 1(a) (each black rectangle is an individual sensor). The substrates were kept at 110 ºC to speed up water evaporation during painting, preventing the formation of circular drying stains, or "coffee rings" pattern, and providing thickness control.

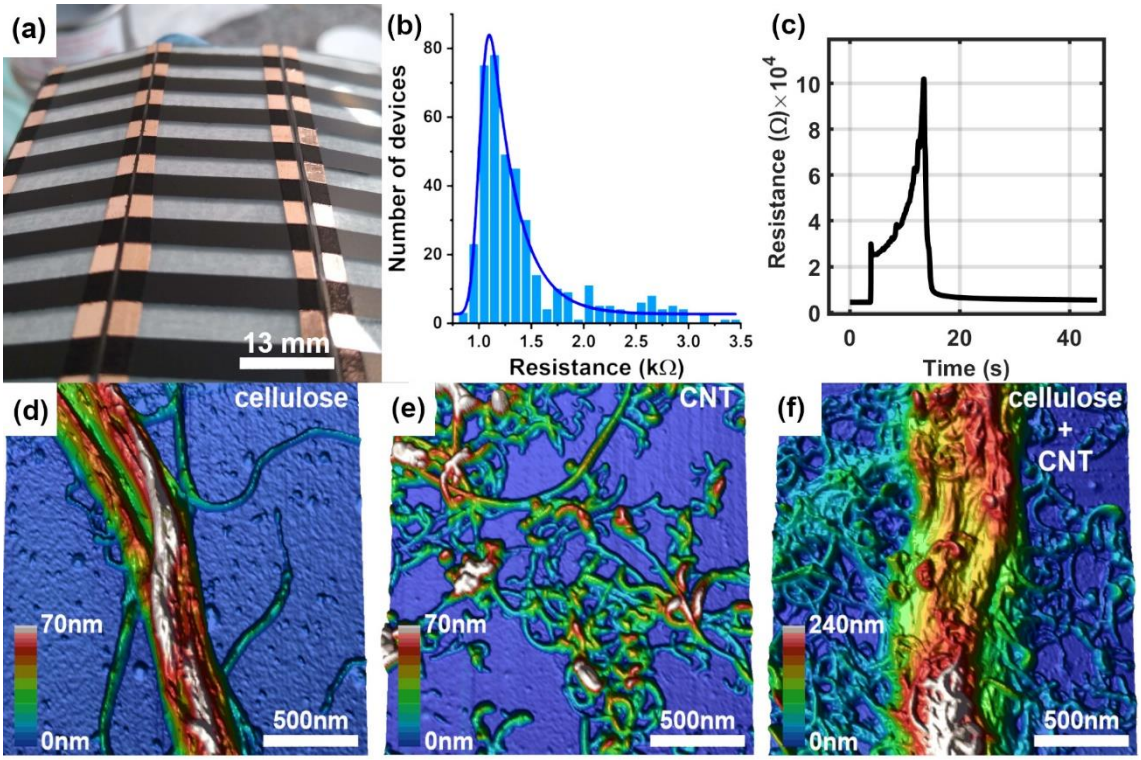

Figure 1 - (a) Array of transducers; (b) histogram of sensor resistance distribution; (c) transducer resistance change as a function of time during liquid sensing; AFM images of (d) micro fibrillated cellulose (MFC), (e) MWCNTs, and (f) MFC entangled with MWCNTs.

After painting, electrical contacts were applied at the ends of each device with conductive silver paint. This method can prepare a series of devices which can be varied by changing the number of painted layers. Figure 1(b) shows a histogram of sensor's initial resistance distribution, where around 400 devices were fabricated and measured, demonstrating the system's robustness for large-scale sensor device production. The resistance distribution was fitted using an exponentially modified Gaussian (EMG) and the calculated mean resistance and standard deviation as $(1{,}26 \pm 0{,}07)\ K\Omega$.

To better understand how the MWCNT and MFC are distributed within the ink, AFM measurements were performed on the isolated materials (MFC and MWCNTs) and on the MFC/MWCNT composite (see Fig. 1(d), 1(e), and 1(f)). Pure MFC fibers form bundles (~ 250 nm-thick), and the functionalized tubes also behave as expected, forming small bundles.

Interestingly, Fig. 1(f) shows that the carbon nanotubes tend to twine around the MFC fiber when mixed. Thus, one can visualize that the composite ink is composed of an insulating matrix of MFC fibers intertwined by a conductive CNT network.

To analyze the data, principal components analysis (PCA) was performed. PCA is a multivariate technique that transform several variables correlated with each other in a new set of orthogonal variables (the principal components) to extract and condense the variance information of all set in just two or three components, showing the similarities and differences between the classes in the set [60].

3 Results and discussions

3.1 Liquid analysis

3.1.1 Detection of glycerin in water

The liquid sensing measurements were performed by applying a fixed voltage (5 V) on the device while collecting the current (I) as a function of time. 6.5 µL of the tested liquid is dripped onto the transducers, while the current is monitored until the complete evaporation of the liquid. The device temperature is kept just below the liquid's boiling point under evaluation. Afterward, the current is used to calculated the resistance, R_0 (see Fig. 1(c)), and a sensitivity gain (S) defined as $S = (R - R_0)/R_0$, where R_0 is the sensor initial resistance, as fabricated, and R is the actual resistance. Features of the experimental curves such as area, maximum peak value, peak width, among others, were used as input parameters and are described in detail in the supplementary information. We analyzed two different liquid groups in the present work: low concentration glycerin/DI-water mixtures (10 ppm and 100 ppm) and a set of organic solvents (DI-water, isopropyl, toluene, ethyl alcohol, chloroform, and ethyl alcohol).

To probe the limit of detection of the MFC/MWCNT composite, we performed measurements of glycerin in water at ppm concentration ranges, with the sensor temperature

set to 95 ºC. Since glycerin does not evaporate at 95ºC, it leaves residues in the sensor matrix, preventing the same sensor device to be used in successive measurements. Thus, in this case a single (drop) measurement was performed for each individual sensor. The parameters analyzed by PCA were *max, t_max, slope, and ratio_maxmin* (defined in Supplementary information as the input features). Fig. 2(a) and (b) depict the sensitivity gain S for pure water, 10 ppm and 100 ppm of glycerin in water and the PCA analysis for this system. The sensor was able to distinguish these three cases, demonstrating both robustness and sensitiveness of the MFC/MWCNT composite as a low concentration oil sensor.

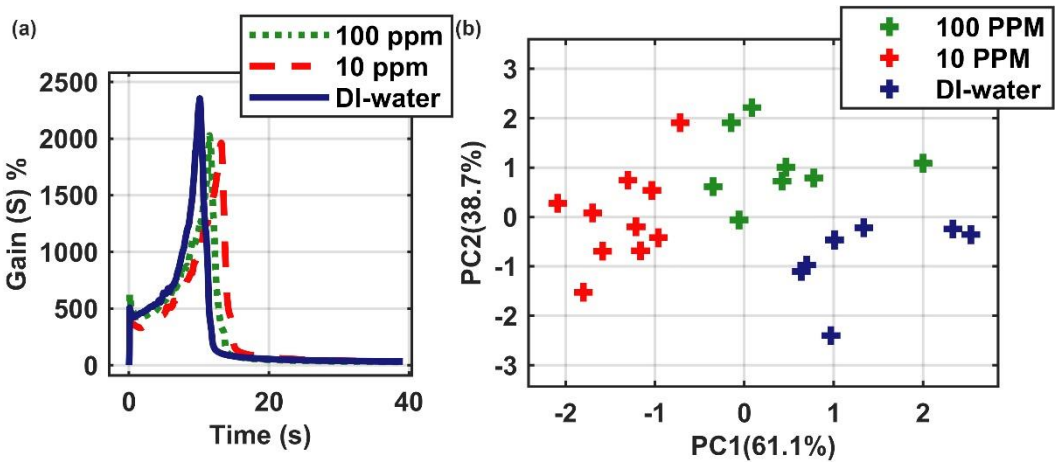

Figure 2 - (a) Gain curves obtained from different glycerin/water mixtures; Each point at the PCA diagram (Fig 2.b) was calculated from a single measurement. (b) PCA analysis of DI-water, 10 ppm and 100 ppm glycerin/water mixture.

3.2 Organic solvents recognition

The MFC/MWCNT transducer was also evaluated for organic solvent recognition. The electrical response of DI-water, isopropyl, toluene, ethyl alcohol, chloroform and ethyl alcohol are shown in figure 3(a). Due to the broad spectra of solvents tested, we set the device

temperature to 55ºC to prevent instantaneous evaporation of the more volatile solvents. Each MFC/MWCNT transducer was used just once to prevent contamination effects. Fig. 3(a) and (b) show gain as a function of time and the PCA analysis for all solvents, respectively. Again, all solvents were easily discriminated via PCA analysis. In this case, the parameters used for PCA analysis were *Area, and FWHM with* $\lambda = 0.50$ (see Supplementary information for more information).

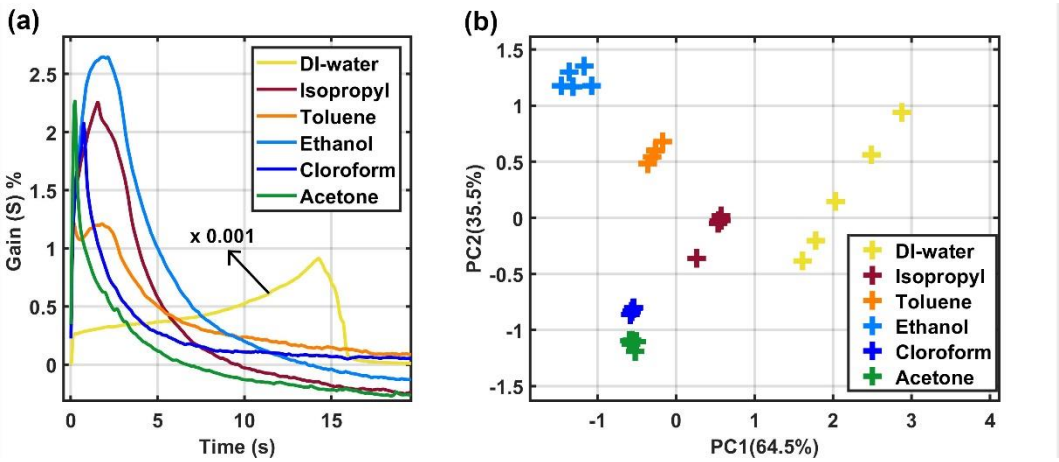

Figure 3 - (a) Gain curves obtained from different organic solvents. (b) PCA analysis of organic solvents showing excellent distinction between the sample categories. Ps. in the case of DI-water, a scale factor of (x 0.001) was applied to the curve of figure 3(a) to help visualization.

4 Electronic tongue mechanisms

Fig. 4(a) shows the step-by-step liquid behavior (as a function of time) as it gets in contact with the transducer. Initially, the composite is dry, at a constant temperature, and traversed by a constant current (red part). As a drop gets in touch with the composite, the electrical current rapidly decreases and the system starts losing heat as the liquid gets absorbed in the entangled composite matrix. This effect reduces the percolation between the conductive MWCNT clusters, generating an increase in gain (resistance) and decreasing the current (pink part). The absorbed liquid keeps swelling the material while it simultaneously absorbs heat and evaporates (blue part). At a certain point, the evaporation leads to drying of the composite, reversing the swelling process, decreasing gain until it reaches a point close to its initial value (green part).

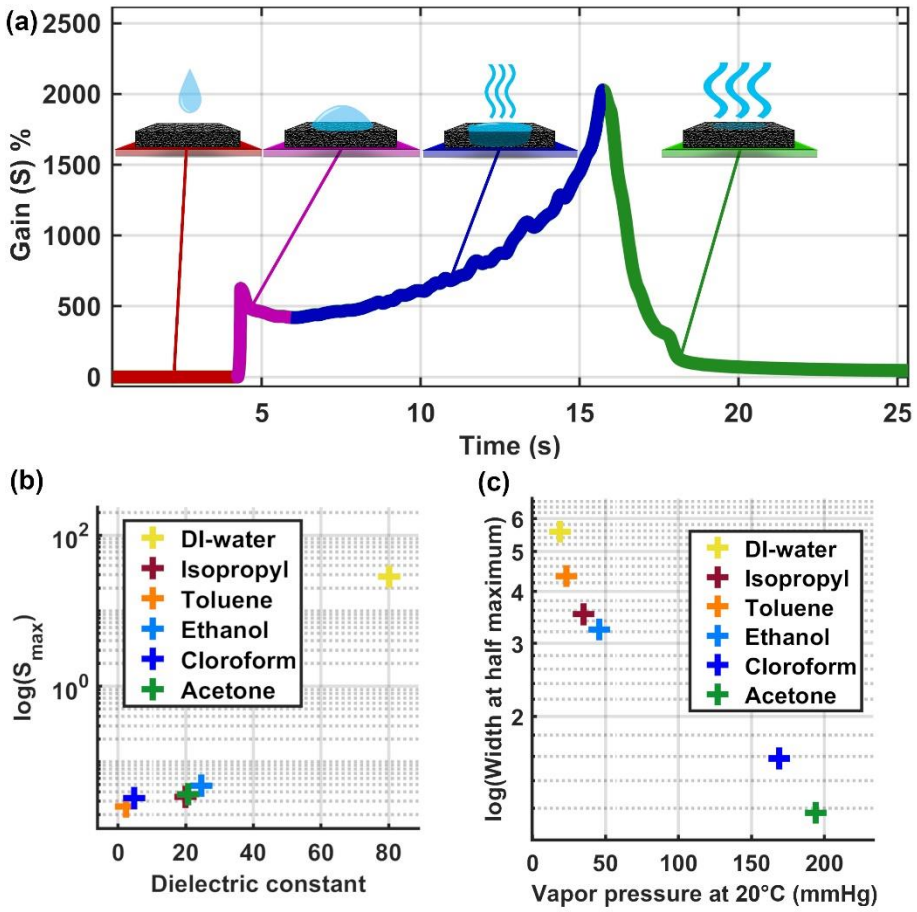

Figure 4 – (a) Sketch depicting a step-by-step process of the sensing dynamics. (b) Correlation between the dielectric constant of the tested solvents and the maximum gain obtained from the Gain curves shown in figure 3. (c) Correlation between the vapor pressure of the tested solvents and the width at half maximum (FWHM) obtained from the Gain curves shown in figure 3.

In order to understand the nature of the interaction between the transducer and the liquids, we correlated the main variables used for PCA analysis (*maximum gain* and width at half-maximum (FWHM) as described in supplementary information) with the physicochemical organic solvent properties (vapor pressure and dielectric constant). Guided by previous studies that show the electrical response is due to the swelling behavior of CPCs [55,56,61], we found that the maximum value in the gain curve (*max*) is proportional to the Dielectric constant of the solvent as shown in Fig 4(b)**.** This result suggests that, when the liquid soaks the composite, it swells the material, creating a liquid dielectric barrier between the conductive clusters. Thus, it changes the tunneling process proportionally to the liquid media dielectric constant. Hence, our results demonstrate that the dielectric constant has an essential role in the sensing mechanism with a clear correlation with the maximum gain of the sensor.

On the other hand, the width of the curves seems to be strongly influenced by the thermal properties of the liquids. As shown in Fig 4(c), the vapor pressure of the solvents controls the time the liquid will stay within the sensor before it evaporates, being a key factor to maintain the swelling process of the CPC matrix and changing the electron tunneling process as explained. To investigate this hypothesis, we designed an experiment to mimic the thermal effects produced by the impinging liquid drops over the heated surface of the transducer. The temperature change and the heat flow produced by the liquid, as it gets in contact with the heated surface, was estimated by dripping a liquid (of about 6.5 µL) onto an

empty crucible kept at 55 ºC inside a thermogravimetric analyzer. The system was monitored until the complete evaporation of the liquid, resulting in the curves shown in figure 5(a).

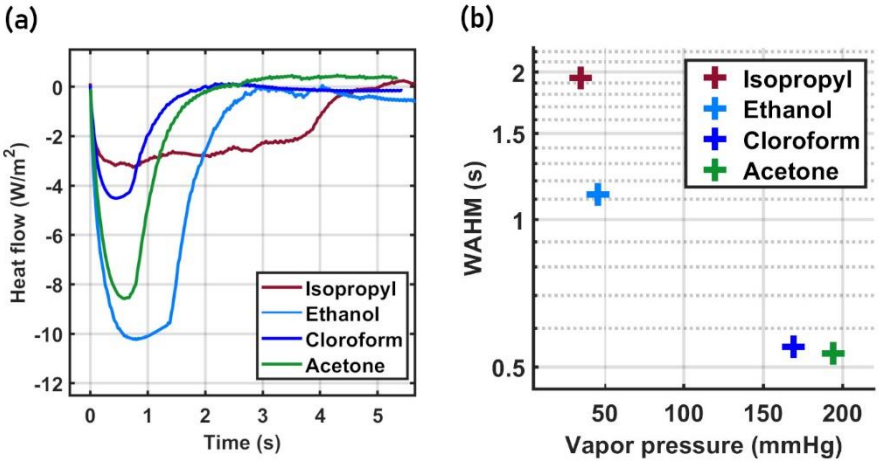

Figure 5 – (a) Heat flow behavior of different solvents (b) Correlation between the width at half maximum (FWHM) and the vapor pressure of the tested solvents.

The thermal behavior of acetone, chloroform, ethanol and isopropyl alcohol exhibit significant similarities with the electrical curves presented in Fig. 3(a), especially regarding the width of the peaks. The interaction of the liquid with the hot crucible is analogous to the interaction of the liquid with the transducer from the thermal point of view. In both cases, the contact of the liquid with the hot surface causes a temperature drop due to the heat transfer from the surface to the fluid. However, as the liquid reaches thermal equilibrium with the surface (minimum point), the heat flow changes direction and the temperature of the system increases, favoring the evaporation of the fluid. Thus, in Fig. 5(b), we observe a strong correlation between the width of the heat flow curves and the vapor pressure of the liquids. We observed the same correlation for the device curves presented in Fig. 4(c), evidencing the role of the thermal proprieties of the liquids as a critical component of the sensor electrical response.

5 Conclusions

In this work, a liquid sensor was developed based on a MFC/MWCNT composite that can be easily scalable manufactured by printing techniques. AFM measurements show that the composite coating is formed by a MFC fiber insulating matrix decorated with a conductive CNT network. The sensor response for different liquids and solvents is fast (40 s) and highly reproducible. The glycerin/water experiment shows sensitivity to detect oil compounds down to the PPM range. Also, we demonstrate the important role of the dielectric constant and vapor pressure on the transduction mechanism of MFC/MWCNTs composite. We believe that our sensor can overcome the scale-up and reproducibility limitations of other liquid sensor devices and have great potential to be applied in various industrial fields for liquid monitoring.

ACKNOWLEDGEMENTS

The authors also would like to thank Fapemig (Rede 2D and individual projects), INCT Nanomateriais de Carbono, CNPq /MCT, Petrobras, BNDES and CAPES for the funding support. We are also thankful to LabNano, Laboratório de Cristalografia (LabCri), CT-NANO-UFMG, and SISNANO/LCPNano at UFMG. APMB acknowledges financial support from CNPq, Fapemig and UFOP - Grant Custeio. We also would like to acknowledge Vinicius Castro and Dra. Glaura Silva at CTNANO for providing the functionalized carbon nanotubes materials. We also would like to acknowledge Douglas Miquita and Centro de Microscopia-UFMG for providing the SEM and TEM images included in the Supporting information.

References:

(1) Akinwande, D. *Nat Nanotechnol* **2017**, *12*, 287–288. doi:10.1038/nnano.2017.65

(2) Gao, W.; Emaminejad, S.; Nyein, H. Y. Y.; Challa, S.; Chen, K.; Peck, A.; Fahad, H. M.; Ota, H.; Shiraki, H.; Kiriya, D.; Lien, D.-H.; Brooks, G. A.; Davis, R. W.; Javey, A. *Nature* **2016**, *529*, 509–514. doi:10.1038/nature16521

(3) Lipomi, D. J.; Vosgueritchian, M.; Tee, B. C.-K.; Hellstrom, S. L.; Lee, J. A.; Fox, C. H.; Bao, Z. *Nat Nanotechnol* **2011**, *6*, 788–792. doi:10.1038/nnano.2011.184

(4) Liu, X.; Gu, L.; Zhang, Q.; Wu, J.; Long, Y.; Fan, Z. *Nat Commun* **2014**, *5*. doi:10.1038/ncomms5007

(5) Yeom, C.; Chen, K.; Kiriya, D.; Yu, Z.; Cho, G.; Javey, A. *Advanced Materials* **2015**, *27*, 1561–1566. doi:10.1002/adma.201404850

(6) Mimendia, A.; Gutiérrez, J. M.; Leija, L.; Hernández, P. R.; Favari, L.; Muñoz, R.; del Valle, M. *Environmental Modelling & Software* **2010**, *25*, 1023–1030. doi:10.1016/j.envsoft.2009.12.003

(7) Campos, I.; Alcañiz, M.; Aguado, D.; Barat, R.; Ferrer, J.; Gil, L.; Marrakchi, M.; Mart\'\inez-Mañez, R.; Soto, J.; Vivancos, J.-L. *Water Res* **2012**, *46*, 2605–2614. doi:10.1016/j.watres.2012.02.029

(8) de Queiroz, D. P.; de Oliveira Florentino, A.; Bruno, J. C.; da Silva, J. H. D.; Riul, A.; Giacometti, J. A. *Sens Actuators B Chem* **2016**, *230*, 566–570. doi:10.1016/j.snb.2016.02.080

(9) Liu, M.; Wang, M.; Wang, J.; Li, D. *Sens Actuators B Chem* **2013**, *177*, 970–980. doi:10.1016/j.snb.2012.11.071

(10) Masson, P. *J Chromatogr A* **2007**, *1158*, 168–173. doi:10.1016/J.CHROMA.2007.03.003

(11) Petrović, M.; Hernando, M. D.; Díaz-Cruz, M. S.; Barceló, D. *J Chromatogr A* **2005**, *1067*, 1–14. doi:10.1016/J.CHROMA.2004.10.110

(12) Singh, R.; Singh, E.; Nalwa, H. S. *{RSC} Adv.* **2017**, *7*, 48597–48630. doi:10.1039/c7ra07191d

(13) Cardenas, J. A.; Andrews, J. B.; Noyce, S. G.; Franklin, A. D. *Nano Futures* **2020**, *4*, 12001. doi:10.1088/2399-1984/ab5f20

(14) Villmow, T.; Pegel, S.; John, A.; Rentenberger, R.; Pötschke, P. *Materials Today* **2011**, *14*, 340–345. doi:10.1016/s1369-7021(11)70164-x

(15) Casiraghi, C.; Macucci, M.; Parvez, K.; Worsley, R.; Shin, Y.; Bronte, F.; Borri, C.; Paggi, M.; Fiori, G. *Carbon N Y* **2018**, *129*, 462–467. doi:10.1016/j.carbon.2017.12.030

(16) Ciosek, P.; Wróblewski, W. *Analyst* **2007**, *132*, 963. doi:10.1039/b705107g

(17) del Valle, M. *International Journal of Electrochemistry* **2012**, *2012*, 1–11. doi:10.1155/2012/986025

(18) Jr., A. R.; Dantas, C. A. R.; Miyazaki, C. M.; Jr., O. N. O. *Analyst* **2010**, *135*, 2481. doi:10.1039/c0an00292e

(19) Atzori, L.; Iera, A.; Morabito, G. *Computer Networks* **2010**, *54*, 2787–2805. doi:10.1016/j.comnet.2010.05.010

(20) Shimizu, F. M.; Pasqualeti, A. M.; Todão, F. R.; de Oliveira, J. F. A.; Vieira, L. C. S.; Gonçalves, S. P. C.; da Silva, G. H.; Cardoso, M. B.; Gobbi, A. L.; Martinez, D. S. T.; Oliveira, O. N.; Lima, R. S. *ACS Sens* **2018**, *3*, 716–726. doi:10.1021/acssensors.8b00056

(21) Moya, A.; Gabriel, G.; Villa, R.; del Campo, F. J. *Curr Opin Electrochem* **2017**, *3*, 29–39. doi:10.1016/j.coelec.2017.05.003

(22) Podrażka, M.; B\.aczyńska, E.; Kundys, M.; Jeleń, P.; Nery, E. W. *Biosensors (Basel)* **2017**, *8*, 3. doi:10.3390/bios8010003

(23) Oliveira, J. E.; Grassi, V.; Scagion, V. P.; Mattoso, L. H. C.; Glenn, G. M.; Medeiros, E. S. *IEEE Sens J* **2013**, *13*, 759–766. doi:10.1109/jsen.2012.2226715

(24) Facure, M. H. M.; Mercante, L. A.; Mattoso, L. H. C.; Correa, D. S. *Talanta* **2017**, *167*, 59–66. doi:10.1016/j.talanta.2017.02.005

(25) Villmow, T.; Pegel, S.; Pötschke, P.; Heinrich, G. *Polymer (Guildf)* **2011**, *52*, 2276–2285. doi:10.1016/j.polymer.2011.03.029

(26) Pioggia, G.; Francesco, F. di; Ferro, M.; Sorrentino, F.; Salvo, P.; Ahluwalia, A. *Microchimica Acta* **2008**, *163*, 57–62. doi:10.1007/s00604-008-0952-y

(27) Lin, Y.; Dong, X.; Liu, S.; Chen, S.; Wei, Y.; Liu, L. *ACS Appl Mater Interfaces* **2016**, *8*, 24143–24151. doi:10.1021/acsami.6b08587

(28) Zhang, K.; Yu, H.-O.; Shi, Y.-D.; Chen, Y.-F.; Zeng, J.-B.; Guo, J.; Wang, B.; Guo, Z.; Wang, M. *J Mater Chem C Mater* **2017**, *5*, 2807–2817. doi:10.1039/c7tc00389g

(29) Al-Oqla, F. M.; Sapuan, S. M.; Anwer, T.; Jawaid, M.; Hoque, M. E. Natural Fiber Reinforced Conductive Polymer Composites as Functional Materials: A Review. *Synthetic Metals*. 2015. doi:10.1016/j.synthmet.2015.04.014

(30) Kafy, A.; Sadasivuni, K. K.; Akther, A.; Min, S.-K.; Kim, J. *Mater Lett* **2015**, *159*, 20–23. doi:10.1016/j.matlet.2015.05.102

(31) McManus, D.; Santo, A. D.; Selvasundaram, P. B.; Krupke, R.; LiBassi, A.; Casiraghi, C. *Flexible and Printed Electronics* **2018**, *3*, 34005. doi:10.1088/2058-8585/aaddb5

(32) Gao, K.; Shao, Z.; Wu, X.; Wang, X.; Li, J.; Zhang, Y.; Wang, W.; Wang, F. *Carbohydr Polym* **2013**, *97*, 243–251. doi:10.1016/j.carbpol.2013.03.067

(33) Jiang, X.; Yang, T.; Li, C.; Zhang, R.; Zhang, L.; Zhao, X.; Zhu, H. *Global Challenges* **2017**, *1*, 1700037. doi:10.1002/gch2.201700037

(34) Gnanaseelan, M.; Chen, Y.; Luo, J.; Krause, B.; Pionteck, J.; Pötschke, P.; Qi, H. *Compos Sci Technol* **2018**, *163*, 133–140. doi:10.1016/j.compscitech.2018.04.026

(35) Yun, S.; Kim, J. *Sens Actuators B Chem* **2010**, *150*, 308–313. doi:10.1016/j.snb.2010.06.068

(36) Salajkova, M.; Valentini, L.; Zhou, Q.; Berglund, L. A. *Compos Sci Technol* **2013**, *87*, 103–110. doi:10.1016/j.compscitech.2013.06.014

(37) Qi, H.; Liu, J.; Pionteck, J.; Pötschke, P.; Mäder, E. *Sens Actuators B Chem* **2015**, *213*, 20–26. doi:10.1016/j.snb.2015.02.067

(38) Imai, M.; Akiyama, K.; Tanaka, T.; Sano, E. *Compos Sci Technol* **2010**, *70*, 1564–1570. doi:10.1016/j.compscitech.2010.05.023

(39) Qi, H.; Mäder, E.; Liu, J. *Sens Actuators B Chem* **2013**, *185*, 225–230. doi:10.1016/j.snb.2013.04.116

(40) Worsley, R.; Pimpolari, L.; McManus, D.; Ge, N.; Ionescu, R.; Wittkopf, J. A.; Alieva, A.; Basso, G.; Macucci, M.; Iannaccone, G.; Novoselov, K. S.; Holder, H.; Fiori, G.; Casiraghi, C. *ACS Nano* **2018**, *13*, 54–60. doi:10.1021/acsnano.8b06464

(41) McManus, D.; Vranic, S.; Withers, F.; Sanchez-Romaguera, V.; Macucci, M.; Yang, H.; Sorrentino, R.; Parvez, K.; Son, S. K.; Iannaccone, G.; Kostarelos, K.; Fiori, G.; Casiraghi, C. *Nat Nanotechnol* **2017**. doi:10.1038/nnano.2016.281

(42) Mirica, K. A.; Azzarelli, J. M.; Weis, J. G.; Schnorr, J. M.; Swager, T. M. *Proceedings of the National Academy of Sciences* **2013**, *110*, E3265--E3270. doi:10.1073/pnas.1307251110

(43) Gou, P.; Kraut, N. D.; Feigel, I. M.; Bai, H.; Morgan, G. J.; Chen, Y.; Tang, Y.; Bocan, K.; Stachel, J.; Berger, L.; Mickle, M.; Sejdić, E.; Star, A. *Sci Rep* **2014**, *4*. doi:10.1038/srep04468

(44) Kim, T.; Song, H.; Ha, J.; Kim, S.; Kim, D.; Chung, S.; Lee, J.; Hong, Y. *Appl Phys Lett* **2014**, *104*, 113103. doi:10.1063/1.4868633

(45) Tortorich, R.; Choi, J.-W. *Nanomaterials* **2013**, *3*, 453–468. doi:10.3390/nano3030453

(46) da Costa, T. H.; Song, E.; Tortorich, R. P.; Choi, J.-W. *{ECS} Journal of Solid State Science and Technology* **2015**, *4*, S3044--S3047. doi:10.1149/2.0121510jss

(47) George, J.; Abdelghani, A.; Bahoumina, P.; Tantot, O.; Baillargeat, D.; Frigui, K.; Bila, S.; Hallil, H.; Dejous, C. *Sensors* **2019**, *19*, 1768. doi:10.3390/s19081768

(48) Yun, J.-H.; Chang-Soo, H.; Kim, J.; Song, J.-W.; Shin, D.-H.; Park, Y.-G. Fabrication of Carbon Nanotube Sensor Device by Inkjet Printing. In *2008 3rd {IEEE} International Conference on Nano/Micro Engineered and Molecular Systems*; IEEE, 2008. doi:10.1109/nems.2008.4484382

(49) Liang, B.; Zhang, Z.; Chen, W.; Lu, D.; Yang, L.; Yang, R.; Zhu, H.; Tang, Z.; Gui, X. *Nanomicro Lett* **2019**, *11*. doi:10.1007/s40820-019-0323-8

(50) Soum, V.; Park, S.; Brilian, A. I.; Kim, Y.; Ryu, M. Y.; Brazell, T.; Burpo, F. J.; Parker, K. K.; Kwon, O.-S.; Shin, K. *ACS Omega* **2019**, *4*, 8626–8631. doi:10.1021/acsomega.9b00936

(51) Lorwongtragool, P.; Sowade, E.; Dinh, T. N.; Kanoun, O.; Kerdcharoen, T.; Baumann, R. R. Inkjet Printing of Chemiresistive Sensors Based on Polymer and Carbon Nanotube Networks. In *International Multi-Conference on Systems, Sygnals & Devices*; IEEE, 2012. doi:10.1109/ssd.2012.6198043

(52) Tortorich, R. P.; Song, E.; Choi, J.-W. *J Electrochem Soc* **2013**, *161*, B3044--B3048. doi:10.1149/2.008402jes

(53) Shimoni, A.; Azoubel, S.; Magdassi, S. *Nanoscale* **2014**, *6*, 11084–11089. doi:10.1039/c4nr02133a

(54) Qin, Y.; Kwon, H. J.; Subrahmanyam, A.; Howlader, M. M. R.; Selvaganapathy, P. R.; Adronov, A.; Deen, M. J. *Mater Lett* **2016**. doi:10.1016/j.matlet.2016.04.048

(55) Kobashi, K.; Villmow, T.; Andres, T.; Pötschke, P. *Sens Actuators B Chem* **2008**. doi:10.1016/j.snb.2008.06.035

(56) Pötschke, P.; Kobashi, K.; Villmow, T.; Andres, T.; Paiva, M. C.; Covas, J. A. *Compos Sci Technol* **2011**. doi:10.1016/j.compscitech.2011.05.019

(57) Castro, V.; Costa, I.; Medeiros, F.; Siqueira, É.; Kasama, A.; Figueiredo, K.; Lavall, R.; Silva, G.; Castro, V. G.; Costa, I. B.; Medeiros, F. S.; Siqueira, É. J.; Kasama, A. H.; Figueiredo, K. C. S.; Lavall, R. L.; Silva, G. G. *J Braz Chem Soc* **2019**, *30*, 2477–2487. doi:10.21577/0103-5053.20190166

(58) Kunadian, I.; Andrews, R.; Qian, D.; Pinar Mengüç, M. *Carbon N Y* **2009**, *47*, 384–395. doi:10.1016/j.carbon.2008.10.022

(59) da Cunha, T. H. R.; de Oliveira, S.; Martins, I. L.; Geraldo, V.; Miquita, D.; Ramos, S. L. M.; Lacerda, R. G.; Ladeira, L. O.; Ferlauto, A. S. *Carbon N Y* **2018**, *133*, 53–61. doi:10.1016/J.CARBON.2018.03.014

(60) Abdi, H.; Williams, L. J. Principal Component Analysis. *Wiley Interdisciplinary Reviews: Computational Statistics*. 2010. doi:10.1002/wics.101

(61) Villmow, T.; Pegel, S.; Pötschke, P.; Heinrich, G. *Polymer (Guildf)* **2011**. doi:10.1016/j.polymer.2011.03.029